HHS Public Access

Author manuscript

Acta Biomater. Author manuscript; available in PMC 2016 November 01.

Published in final edited form as:

Acta Biomater. 2015 November ; 27: 205–213. doi:10.1016/j.actbio.2015.09.010.

Biological Thiols-Triggered Hydrogen Sulfide Releasing Microfibers for Tissue Engineering Applications

Sheng Feng[1], **Yu Zhao**[2], **Ming Xian**[2,**], and **Qian Wang**[1,*]

[1]Department of Chemistry and Biochemistry and Nanocenter, University of South Carolina, Columbia, SC 29208, USA

[2]Department of Chemistry, Washington State University, Pullman, Washington, 99164, USA

Abstract

By electrospinning of polycaprolactone (PCL) solutions containing N-(benzoylthio)benzamide (NSHD1), a H_2S donor, fibrous scaffolds with hydrogen sulfide (H_2S) releasing capability (H_2S-fibers) are fabricated. The resultant microfibers are capable of releasing H_2S upon immersion in aqueous solution containing biological thiols under physiological conditions. The H_2S release peaks of H_2S-fibers appeared at 2~4 hours, while the peak of donor alone showed at 45 minutes. H_2S release half-lives of H_2S-fibers were 10–20 times longer than that of donor alone. Furthermore, H_2S-fibers can protect cells from H_2O_2 induced oxidative damage by significantly decreasing the production of intracellular reactive oxygen species (ROS). Finally, we investigated the H_2S-fibers application as a wound dressing in *vitro*. Given that H_2S has a broad range of physiological functions, H_2S-fibers hold great potential for various biomedical applications.

Graphical abstract

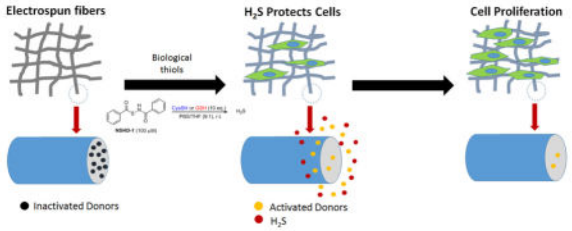

Keywords

hydrogen sulfide; controlled release; electrospinning; NSHD1; ischemia reperfusion injury

**Corresponding author Tel: +1 509 335-6073; Fax: +1 509 335 8086;. *Corresponding author Tel: +1 803 777 8436; Fax: +1 803 777 9521; mxian@wsu.edu (M. Xian); wang263@mailbox.sc.edu (Q. Wang).

Introduction

Hydrogen sulfide (H_2S) has long been considered as a malodorous toxic gas. Abe and Kimura first reported the possible role of endogenous H_2S in the neuromodulation [1], indicating the biological relevance of H_2S as a gasotransmitter. Together with nitric oxide (NO) and carbon monoxide (CO), H_2S forms part of a group of active gaseous molecules that modulate cellular functions through intracellular signaling cascades [2]. Most, if not all, of endogenous formation of H_2S is attributed to four enzymes, cystathionine β-synthase (CBS), cystathionine γ-lyase (CSE), and the tandem enzymes cysteine aminotransferase (CAT) and 3-mercaptopyruvate sulfurtransferase (3-MST) [3–5]. Tightly controlled endogenous H_2S has involved in diverse physiological and pathophysiological processes, including learning and memory, neurodegeneration, regulation of inflammation and blood pressure, metabolism, and anti-apoptosis [6]. Possessing all positive effects of NO without generating a toxic metabolite such as $ONOO^-$ [7], H_2S holds great therapeutic potential for various diseases and has drawn increased attention of biomedical scientists.

Limited available H_2S releasing agents (i.e. H_2S donors), such as sulfide salts, natural polysulfide compounds such as diallyl trisulfide, synthetic H_2S donors such as Lawesson's reagent derivative, GYY4137, have been developed and applied for the studies of the physiological and pathological functions of H_2S [8]. Recently, a polymeric H_2S donor synthesized by conjugating 5-(4-hydroxyphenyl)-3H-1,2-dithiole-3-thione (ADT-OH) to polymers showed effects of potentiating lipopolysaccharide-induced inflammation and altered cellular trafficking [9]. However, the shortage of aforementioned H_2S donors is that the H_2S release is either too fast or uncontrollable, which poorly mimic the biological generation of H_2S. For example, sulfide salts Na_2S and NaHS, as the most widely used H_2S donor, have a fast and spontaneous H_2S release in aqueous solutions. H_2S gas concentration reaches a maximum within 20 seconds and falls exponentially thereafter [10]. Other commonly used H_2S donors, such as GYY4137 [11], polysulfide such as diallyl disulfide (DADS) and diallyl trisulfide (DATS) [12], ADT-OH [13], and thioamides [14] have peaking times ranging from several minutes up to 15 minutes. To overcome this drawback, we have developed a series of *N*-(benzoylthio)benzamides derivatives (NSHD), which are controllable and have a relative slow-releasing profile [15]. The H_2S release of these donors can be triggered by biological thiols such as cysteine and glutathione (GSH), which are prevail in the biological system. Therefore, NSHDs are promising candidates for H_2S-based therapeutic strategy.

Electrospinning is a simple, cost-effective, and versatile technique in which natural or synthetic polymers are fabricated into fibers with diameters ranging from tens nanometers to micrometers. The unique advantages, such as high surface to volume ratio, adjustable porosity, and the flexibility to form various sizes, make the electrospun fibers an ideal system for a broad range of biomedical applications, such as wound dressing, blood vessel tissue engineering, neural repair, bone or cartilage tissue engineering, and controlled drug release, as described in several reviews [16–18]. Previously, researchers have functionalized electrospun fibers with biological relevant macromolecules, such as low molecular weight heparin [19], growth factor bone morphogenetic protein 2 (BMP2) [20], neural growth factor [21], and specific genes [22]. Notably, several groups have generated electrospun

fibers with capability to release gaseous messenger nitric oxide [23–27]. Though emerging role of H_2S in physiological and pathophysiological processes indicates H_2S holds great therapeutic potential [28], to the best of our knowledge, no H_2S-releasing electrospun fibers (H_2S-fibers) has been generated and evaluated so far.

Fibrous scaffolds generated by electrospinning have been used to generate substitutes and grafts for various tissue regeneration and achieved significant progress [17]. The electrospun fibers served as cell scaffolds for the therapeutic cells to adhere, proliferate, and differentiation, in the damaged tissues or organs [16]. However, in the process of transplantation of organs, tissue substitutes, and therapeutic cells, ischemia *in vitro* and post-transplantation is the most well-known cause of malfunction of transplanted grafts [29, 30]. Since the production of endogenous H_2S and the exogenous administration of H_2S elicit a wide range of protective actions, especially in cardiovascular systems, including vasodilation, anti-inflammatory, antioxidant, and down regulation of cellular metabolism under stress [28, 31], H_2S-fibers would enhance the regenerative capacity of tissue engineering grafts by protecting surrounding cells from ischemia.

We hypothesized that electrospinning biodegradable polymers doped with a H_2S donor (NSHD1) will generate H_2S-fibers with a controllable slow-releasing profile, which could be used as cell scaffolds to protect cell from ischemia reperfusion injury. To test this hypothesis, we fabricated H_2S-fibers by electrospinning biodegradable polycaprolactone solution containing NSHD1. The resultant H_2S-fibers not only supported the growth of cardiac myoblasts H9c2 and fibroblast NIH 3T3, but also protected cells from hydrogen peroxide (H_2O_2) induced oxidative damage by releasing H_2S. Given the broad biological functions of H_2S, we anticipate this H_2S-releasing scaffold will have great potential for biomedical applications.

Materials and Methods

Electrospinning of H_2S-releasing Fibers

Poly(ε-caprolactone) (PCL) (Average Mn ca. 70–90 kDa, Sigma) were dissolved in 1,1,1,3,3,3-hexafluro-2-propanol (HFIP) (Sigma Aldrich) to obtain 1 to 12% w/w solutions. For samples containing dopant, the polymer was dissolved in HFIP first, followed by the addition of NSHD1. Each polymer solution was drawn into fibers by a home-made electrospinning system described before [32]. Briefly, the polymer solution was transferred to a 1.0 mL plastic syringe (BD) with a 21 G blunt needle (BD precision glide). A syringe driver was used to control the solution flow rate at 15 μL min^{-1}. A high voltage supply (HVR Orlando, FL) was used to build up a voltage of 6–7 kV electric filed between the needle and the grounded collector. The distance between the collector and needle was fixed at 10 cm. The temperature of the electrospinning environment was 25 ° C, and the humidity was below 1%. The random fibers were obtained by using a stationary collector. And the aligned fibers were obtained by using a rotating drum (12 cm in diameter) as the collector. The rotating rate was 1000 revolutions per minute.

Fiber Analysis

The morphology of PCL fibrous scaffolds and elemental analysis via EDX were examined by a scanning electron microscopy (SEM, Zeiss Ultra Plus FESEM). Fibrous scaffolds samples were dried with nitrogen, and coated with gold for 40 seconds with Desk II cold sputter coater (Denton Vacuum, Morristown, NJ). To examine the uniformity of the fibrous diameters, several randomly selected areas were imaged. The same condition was used for EDX. Fibrous diameters were measured using ImageJ (National Institutes of Health). Fourier transform infrared spectrometry (FTIR) was conducted on a Shimadzu 8400 FTIR spectrometer in the range of 500–4000 cm^{-1}.

Hydrogen Sulfide Release

Reactions for the measurement of H_2S release kinetics were run in triplicate. In each test, 50 mg fibers samples were immersed in 50 mL PBS (pH 7.4) containing 1 mM cysteine. Reaction aliquots (1.0 mL) were taken to UV-Vis cuvettes containing zinc acetate (100 μL, 1% w/v in H_2O), $FeCl_3$ (200 μL, 30 mM in 1.2 M HCl), and *N*,*N*-dimethyl-1,4-phenylenediamine sulfate (200 μL, 20 mM in 7.2 M HCl) at predetermined time points. Absorbance at 670 nm was measured 20 min thereafter. H_2S concentrations were calculated according to the Na_2S standard curve. To determine the release half-life, 1% w/v zinc acetate was added to the 50 mL PBS containing 50 mg fibers sample. Then reaction aliquots were taken to UV-Vis cuvettes containing $FeCl_3$ (200 μL, 30 mM in 1.2 M HCl), and *N*,*N*-dimethyl-1,4-phenylenediamine sulfate (200 μL, 20 mM in 7.2 M HCl) at predetermined time points. First-order half-life of H_2S release was determined by plotting time vs. ln(1/(1-% released), with $t_{1/2}$ = ln(2)/slope.

Cell Lines and Cell Cultures

The rat cardiomyocyte cell line H9c2 and the immortalized mouse fibroblast cell line NIH 3T3 were purchased from American Type Culture Collection. Both cell lines were maintained in Dulbecco's modified Eagle's medium (DMEM, #D6046, Sigma–Aldrich) supplemented with 10% heat inactivated fetal bovine serum (Hyclone, Thermo Scientific), 100 U mL^{-1} penicillin and 100 μg mL^{-1} streptomycin (Gibco BRL, Invitrogen Corp., Carlsbad, CA, USA). Cells were cultured in a 5% CO_2 humidified incubator at 37 °C. Sterilized PCL fibrous scaffolds were soaked in media 30 min prior cell seeding. Cells in exponential growth phase were trypsinized by 0.25% trypsin and seeded on PCL fibrous scaffold at a density of 5.2×10^3 cells per cm^2.

Cell Viability Assay

Cells growing exponentially were trypsinized and seeded in tissue culture plates and then incubated with NSHD-1 at different concentrations (20 – 160 μM) for 1 h. Cells were then washed with PBS twice to remove extracellular donors and cell viability was measured by the standard CCK-8 assay. For cells in fibrous scaffolds, cells growing exponentially were trypsinized and seeded in fibrous scaffolds in triplicate wells. After 24 hours, the cell viability was analyzed by CellTiter-Blue™ Cell Viability Assay (Promega, Madison, WI). The CellTiter-Blue reagent was added to the medium directly (100 μL per 1 mL medium) and incubated for four hours at 37°C. Fluorescence at 560ex/590em nm filter setting was

measured using a Tecan infinite M200 plate reader (Tecan, Salzburg, Austria). After correction of background fluorescence, the intensity of fluorescence for each sample was normalized by the control. For the assessment of protective effects of H_2S-fibers against oxidative damage, cells were seeded on fibrous scaffolds with medium containing 250 μM L-Cysteine for predetermined time points, then subjected to 400 μM H_2O_2 treatment for 24 hours. After this, CellTiter-Blue was applied to determine the cell viability.

Fluorescence Microscopy

Cells growing exponentially were trypsinized and seeded in fibrous scaffolds. At predetermined time points, cells were rinsed with phosphate buffered saline (PBS) twice and fixed with 4% paraformaldehyde for 20 min at room temperature. Scaffolds with cells were rinsed with PBS. Cells were permeabilized with 0.2% Triton X100 for 10 min. To prevent non-specific labeling, 3% bovine serum albumin (BSA) in PBS were applied as a blocking buffer for 20 min. Actin cytoskeleton was stained with Rhodamine Phalloidin (Cytoskeleton Inc.) (1:200) in a blocking buffer for 20 min, and nuclei were stained with 4′,6-diamidino-2-phenylindole (DAPI) (Invitrogen) in a blocking buffer for 10 min. The fluorescence was visualized and captured under confocal microscope (Olympus IX81) with DAPI filter and Cy3 filter set.

Detection of H_2S in Cells

H9c2 and NIH 3T3 cells were seeded on fibrous scaffolds for 12 hours. The cells were then incubated with a H_2S probe (WSP-5) [33] solution (250 μM in PBS) and surfactant cetrimonium bromide (CTAB) (500 μM) in PBS at 37 °C for 30 min. After the PBS was removed, the fluorescence signal was observed by confocal microscope (Olympus IX81) with Cy5 filter.

Reactive Oxygen Species Detection

H9c2 cells were seeded in fibrous scaffolds for 24 hours, then treated with 400 μM H_2O_2 for 2 hours. Dihydroethidium (DHE, Invitrogen) staining was applied to quantify ROS production. Cells were incubated with 10 μM DHE for 30 min at 37 °C. Images were obtained using confocal microscope (Olympus IX81) with Cy3 filter. The fluorescent intensity of the nuclei was measured in each field by ImageJ.

Statistical analysis

All assays were performed in triplicates unless otherwise stated. All data were indicated as mean ± SEM. Comparisons were done using one-way ANOVA unless otherwise stated. And post hoc analysis was done using Turkey's multiple comparison test. All the statistical analyses were done by GraphPad Prism.

Results and Discussion

2.1. Fabrication of H_2S-fibers

In the present study, the biodegradable polycaprolactone (PCL) is being used because it has been approved by Food Drug Administration (FDA) in specific devices used in human body for various biomedical applications and fabricated into cellular scaffolds for culturing

different types of cells [34]. By simply adjusting PCL concentrations, we fabricated various microstructures, including spheres, beaded fibers and uniform fibers using our home-made electrospinning equipment (Figure S1a). The detailed optimization of electrospinning condition is provided in the suppementary material.

Previous studies suggest altering solution concentrations remain the most convenient and effectively way for tuning the fiber diameters [35]. In order to form uniform fine fibrous structure with different diameters, PCL solutions with concentrations ranging from 6% - 12% were prepared for electrospinning. For generating H_2S-fibers, the H_2S donor, NSHD1, was being added into 12% PCL solutions with various ratio to PCL (2 wt%, 5 wt%, and 10 wt% with respect to PCL). The structure and activation of NSHD1 are shown in Figure 1g. All solutions with various concentration of NSHD1 successfully formed homogeneous fibrous scaffolds with similar diameters (Figure S2). In order to achieve a relatively high drug loading, we chose 10wt% as a constant ratio of NSHD1 to PCL for further experiments. PCL solutions with concentrations of 6%, 9%, and 12% generated homogeneous fibrous scaffolds with diameters of 0.51 ± 0.16, 0.98 ± 0.16, and 1.47 ± 0.18 micron, respectively (Figure 1a–c). In addition, the SEM images showed that H_2S donor/PCL solutions generated H_2S-fibers with uniform morphology (Figure 1d–f). The surfaces were smooth and no crystals were observed, which indicated that the loaded H_2S donors were evenly distributed in the fibers. The fibers formed from H_2S donor/PCL solutions have shown similar diameters as the fibers generated from PCL solution (PCL-fibers) at each of the solution concentrations (Figure 1h).

The energy dispersive X-ray (EDX) spectra were employed to determine the presence of the H_2S donor in the fibrous matrix via detection of sulfur. The data have shown that the presence of sulfur peak in H_2S-fibers, where there is no sulfur peak in PCL-fibers (Figure 2a–b). Furthermore, the Fourier transform infrared spectrometry (FTIR) spectrum was applied to confirm the incorporation of NSHD1 into H_2S-fibers. The FTIR spectra of PCL-fibers showed peaks located at 2945, 2866, and 1723 cm^{-1}, which were assigned to the stretching vibration of –C=O bonds (Figure 2c). The FTIR spectra of the H_2S-fibers showed additional absorption peaks at 3315, 1650, and 690 cm^{-1} compared with the spectra of the PCL-fibers, due to the presence of H_2S donor (Figure 2e). Those additional absorption peaks at 3315, 1650, and 690 cm were attributed to amide N-H stretch, amide N-H bending, and aromatic C-H bending, respectively, which matched the peaks of donor alone (Figure 2d). These data suggested that the donor has been successfully doped into the electrospun fibrous scaffolds.

Since the alignment of various types of cells are essentially important for cells to form proper organization and fulfill biological function, such as parallel arrangement of myotubes [36], biomaterials with anisotropic property are desired in tissue engineering [37]. Using a homemade rotating collector, we generated aligned fibrous scaffolds by electrospinning (Figure S3) [38].

2.2. Hydrogen Sulfide Release

H_2S has recently been recognized as an endogenously generated signaling molecule with potent cytoprotective actions [39]. Although the exact mechanism of action is still under

investigation, the production of endogenous H_2S and the exogenous administration of H_2S elicit a wide range of protective actions, especially in cardiovascular systems, including vasodilation, anti-inflammatory, antioxidant, and down regulation of cellular metabolism under stress [28, 31]. Therefore fabrication of scaffolds capable of releasing H_2S is a promising therapeutic strategy. Here we investigated the H_2S releasing profiles of H_2S-fibers with different fiber diameters. To evaluate the rate of H_2S release from H_2S-fibers or donor alone, we measured H_2S release using two different methods: (1) instantaneous H_2S monitor with zinc acetate being added into each aliquot and (2) cumulative H_2S release with zinc acetate being added into the reacting mixture to estimate the releasing half-lives [40].

As explained previously, our H_2S donor can be activated by biological thiols such as cysteine and GSH. The biological thiols-triggered H_2S donors enable resultant H_2S-fibers carry the advantage of controllable H_2S release. In a study of 106 healthy adults, the plasma thiols, including homocysteine, GSH, and cysteine, were about 300 to 400 μM [41]. Based on our previous study, those free thiols were able to trigger H_2S release of our donors [15]. Since the cysteine is one of the most prevail biological thiols in the plasma and gives fast activation of NSHD1, it was used as the representative activator of H_2S-fibers in the following experiments.

Before investigating the H_2S release kinetics of H_2S-fibers, we first measured the H_2S release of H_2S donor alone. As shown in a typical H_2S release curve of NSHD1 in pH 7.4 phosphate buffer (Figure 3a), the concentration of H_2S released from the donor reached a maximum value at 40 min (the peaking time), and then started to decrease, presumably due to volatilization, which is consistent with previously report [15]. The half-life of the donor for the pseudo-first-order kinetic plots was determined and found to be about 14 min.

Although various H_2S donors have been reported for cellular studies, the fast and uncontrollable H_2S release of those donors compromised their capacity to mimic the physiological generation of H_2S. Compared with donor alone, we expect the H_2S-fibers demonstrate extended H_2S-releasing profiles. Meanwhile, those fibers with different diameters might give different H_2S release kinetics. As our expectation, the peaking times for H_2S-fibers generated from 6%, 9%, and 12% solutions were 120, 160, and 210 min, respectively (Figure 3b). The H_2S releasing half-lives of H_2S fibers from 6%, 9%, and 12% were prolonged approximately 10–50 folds, compared with donor alone. Furthermore, H_2S-fibers generated from 12% solutions demonstrated prolonged and evenly distributed H_2S release, relative to others. These data indicate that H_2S-fibers significantly prolonged H_2S release and might better mimic the biological H_2S generation.

We next investigated the release of NSHD1 from H_2S-fibers. NSHD1 has a UV absorbance peak at λ_{max} = 242 nm. Thus, the amount of NSHD1 released from the fibers was determined by UV spectroscopy using a predetermined calibration curve $C = 91.5751A - 1.5833$ (R = 0.9988) where C is the concentration of NSHD1 (μM) and A is the solution absorbance at 242 nm (Figure S3a–b). The initial burst release followed by the relatively steady release was observed. The burst release was attributed to release of NSHD1 from a superficial area of the electrospun fibers. The smaller diameter fibers exhibited higher burst release feature, which is consistent with previous study [42]. After the initial burst release,

the NSHD1 release of 12% H_2S-fibers were slower than 6% and 9% H_2S-fibers (Figure S4c). This is due to that the larger diameter of 12% H_2S-fibers makes the drug harder to diffuse from the interior of the fibers compared to others. In addition, the higher specific surface areas of 6% and 9% H_2S-fibers are beneficial to drug release. After first 24 hours, the NSHD1 release of all H_2S-fibers reached plateau and in the next 70 hours (Figure S4d), the NSHD1 concentration slowly reduced, this might be due to the hydrolysis of the NSHD1, which has been reported in another H_2S donor with similar structure [40].

Based on the calculation, H_2S-Release capacity of NSHD1 were significantly reduced upon being loaded into fibers. This might be due to multiple reasons. First of all, the high voltages might lead to partially degradation of NSHD1. Secondly, the accessibility of NSHD1 towards the activator (cysteine) were influenced after doped into fibers. Thirdly, when we measured the release kinetics in vitro, the oxidation of the activator would also affect the release kinetics. Further investigation needs to be done to address this issue.

After 48 h incubation in PBS at pH 7.4 with excess of cysteine, the H_2S fibers were subjected to SEM imaging. Compared with the original formation, the fibrous structure of electrospun fibrous scaffolds maintained a 3D fibrous morphology, albeit all the fibers were slightly swollen (Figure 3c–e). This might be because of the chain relaxation of the matrix polymer after incubation in the PBS. Since all the fibrous scaffolds remained stable and maintained the 3D structural feature, the fibrous scaffolds can be applied as tissue engineering scaffolds to support the proliferation of cells after releasing H_2S.

Since 12% solution containing the H_2S donor generates 1.5 micron H_2S-fibers with prolonged and evenly distributed H_2S release. For the cell experiments, 12% polymer solution was chosen for the fabrication of H_2S-fibers. In addition, the aligned H_2S-fibers have shown similar release kinetics to random H_2S-fibers as long as that the fiber diameters maintained the same. The aligned fibers have been reported to promote cellular alignment to potentiate their anisotropic properties [43]. Thus H_2S-fibers with aligned orientation were applied for further investigation of cytoprotection.

2.3. Cytocompatibility of H_2S-fibers

With these H_2S-fibers in hand, we next explored their cytocompatibility. Previous studies revealed H_2S protects cardiac cells from myocardial ischemia reperfusion injury [44, 45]. In an *in vitro* model of cutaneous tissue transplantation, H_2S significantly decreased apoptosis of fibroblasts caused by ischemia reperfusion injury [46]. Given the potential applications of H_2S-fibers in those scenarios, H9c2 cardiac myoblasts and NIH 3T3 fibroblasts were chosen as the representatives for the cytocompatibility test.

Before investigating cytocompatibility of H_2S-fibers, we first tested cytotoxicity of NSHD1 to H9c2 cardiomyoblasts. NSHD1 did not exhibit significant cytotoxicity at low concentrations (< 80 μM). However, the cytotoxicity was observed when higher concentrations (160 μM) of NSHD1 were applied. After H9c2 cells were incubated with NSHD1 (160 μM) in the presence of cysteine (480 μM), NSHD1's cytotoxicity was completed suppressed (Figure S5). Considering that cysteine and GSH are relative rich in living systems, we envision NSHD-induced cytotoxicity could be diminished or avoided.

To investigate cytocompatibility of H_2S-fibers, H9c2 and NIH 3T3 cells were cultured in H_2S-fibers for 24 hours and subsequently examined by CellTiter-Blue assay. We observed 50% reduction of cell viability for H9c2 cells cultured on H_2S-fibers compared to PCL-fibers, when no cysteine was added into the culture medium (Figure 4a). Interestingly, we did not observe cytotoxicity towards NIH 3T3 cells (Figure 4b). However, when being cultured in medium containing 250 μM cysteine, both H9c2 and NIH 3T3 cells on H_2S fibers maintained similar viability with cells on PCL-fibers (Figure 4). These data demonstrated that our H_2S fibers were non-toxic to cells in the presence of biological thiols. Given that the concentration of biological thiols including cysteine, homocysteine, and GSH, is ranging from several hundred micromolar to several milimolar *in vivo* [41], H_2S-fibers might be non-toxic to cells and tissues when they are being used as an implanted scaffolds.

To observe cells in H_2S-fibers, H9c2 cells cultured in the fibrous scaffolds in the presence of 250 μM cysteine at day 1, day 3, and day 5 were stained with phalloidin and DAPI, then observed under fluorescence microscopy (Figure S6). The aligned fibers promoted H9c2 to align along the fiber axis. Previous research suggested that this guided alignment could strongly promote myoblasts formation [47]. In addition, H9c2 cells increased in number during cultured in H_2S-fibers. At day 3 and day 5, H9c2 were found to reach an estimated confluence of 50% and 90%, respectively, indicating that H9c2 proliferated in H_2S-fibers. In addition, we did not observe morphological changes of the cells in H_2S-fibers. Similar results were observed in H9c2 cells cultured in PCL-fibers (Figure S7). Taken together, we conclude that H_2S fibers are cytocompatible and can support the cell proliferation.

2.4. H_2S-fibers Protecting Cells from Oxidative Damage

After examining the cytocompatibility of cells with H_2S-fibers, we then used a selective H_2S probe, WSP-5 [33], to monitor the H_2S in cells cultured in H_2S-fibers. H9c2 cells and NIH 3T3 cells were seeded in the H_2S-fibers for 12 hours in the presence of 250 μM cysteine. Then WSP-5 was applied to monitor the intracellular H_2S. As expected, cells in H_2S-fibers showed enhanced fluorescent signals compared to cells in PCL-fibers (Figure 5). The H_2S signal could be observed even after 24 hours of incubation (Data not shown), indicating a sustained release of H_2S from H_2S-fibers.

Previous study revealed that H_2O_2 is a major player in ischemia reperfusion injury, and ischemia causes a dramatic increase of myocardial H_2O_2 content [48]. Therefore, H_2O_2 has been applied to H9c2 cells as an *in vitro* ischemia model [49]. Recent studies suggested H_2S holds a great potential in protecting cells from ischemia reperfusion injury. To test the biological function of our H_2S-fibers, we evaluated the cytoprotective effect of H_2S-fibers against H_2O_2 induced oxidative damage. We first exposed H9c2 cells to H_2O_2 in a range of 0 to 1000 μM for 24 h in serum free medium. The CellTiter-Blue assay was performed to determine the viability of H9c2 cells treated by H_2O_2. A dose-dependent loss of cell viabilities was observed in H9c2 with concentrations between 100 to 700 μM (Figure 6a). A concentration of 400 μM of H_2O_2 that could reduce 50% cell viability was chosen for later studies. The H9c2 cells and NIH 3T3 cells were seeded in H_2S fibers or PCL fibers for 24 hours with 250 μM cysteine. Then cells in the fibers were switched into serum free medium

containing 400 μM H_2O_2 for 24 hours. The cell viabilities were measured by CellTiter-Blue assay. Our data demonstrated that viabilities of cells in H_2S fibers were significantly higher than ones in PCL-fibers. However, if there was no extra cysteine being added in the culture medium, the cytotoxicity of H_2S-fibers synergized the effect of H_2O_2 to further decrease the cell viabilities (Figure 6b–c). Interestingly, the cells on 3D fibrous scaffolds were more sensitive to H_2O_2 treatment than cells on tissue culture plastics, probably due to the alteration of culture dimensions [50]. The protective effect of H_2S fibers were observed up to 36 hours and disappeared at 48 hours (Figure S8). In the transplantation of stem cells and various organs, the post-transplantational ischemia reperfusion injury, which happens in the first several hours, is the major cause for the malfunction of transplanted grafts [29, 30]. Therefore, our H_2S fibers with a 36 hours protective effect have the potential biomedical application as a tissue engineering scaffold.

Increased generation of reactive oxygen species (ROS) during both ischemia and reperfusion plays an essential role in the pathophysiology of intraoperative myocardial injury [51]. Cardioprotective effect of H_2S during ischemia reperfusion results from decreasing the levels of ROS production [52]. To confirm that our H_2S fibers have the cytoprotective function, we investigated the ROS production of H9c2 cells in H_2S-fibers or PCL-fibers under H_2O_2 treatment. After 2 hours of exposure to H_2O_2, the ROS generation was measured using live cell imaging with a ROS probe, dihydroethidium (DHE) [53]. The intracellular fluorescence intensity in the nuclei, which reflected ROS generation, was significantly lower for cells cultured in H_2S-fibers with 250 μM cysteine than counterparts in PCL-fibers and H_2S-fibers without cysteine (Figure 7). In a control study performed in tissue culture plastics, H9c2 cells pretreated with 160 μM NSHD1 and 480 μM cysteine showed significantly decreased DHE fluorescence signal after 2 h exposure to 400 μM H_2O_2, compared to cells without pretreatment (Figure S9). These data suggest that our H_2S-fibers can effectively protect cells from H_2O_2 induced oxidative injury by releasing H_2S.

2.5. H_2S-fibers for Wound Dressing

We have found that our H_2S-fibers can protect cells from oxidative damage by preventing ROS production. To investigate the potential application of H_2S-fibers for wound dressing, 3T3 fibroblast cell line was chosen as the model cells because the fibroblasts play an essential role in wound healing process, besides keratinocytes. The proliferation of fibroblasts in response to H_2S fibers showed the similar rate as cells cultured in PCL-fibers in 5 days (Figure 8a). This indicates that the H_2S does not affect the proliferation of 3T3 cells, which is an important event necessary for wound healing. Therefore, the H_2S-fibers should be able to protect the cells cultured from the oxidative damages, while maintaining their capacity to support 3T3 proliferation.

Collagen protein is critical for the strength and integrity of extracellular matrix during the wound healing process. [54] In addition, α-SMA is a major player in scarring and fibrosis. [55] Therefore, to investigate the effect of H_2S-fiber on 3T3 cells during wound healing, we measured the expression of collagen type I, collagen type III, and α-SMA by quantitative PCR. We found that 3T3 cells cultured in H_2S-fibers have increased the expression of collagen type I ($P < 0.05$) and collagen type III ($P < 0.05$) (Figure 8b). Clearly the H_2S-

fibers that protect cells from oxidative stress can support the proliferation of fibroblasts and promote the expression of wound healing related genes. We anticipate the H_2S-fibers would be a great candidate for wound dressing application.

3. Conclusions

Hydrogen sulfide has been gaining significant attentions recently due to its broad range of biological functions. Here, combining electrospinning technique with a H_2S donor, we generated fibrous scaffolds with controllable H_2S release. By adjusting fiber diameters, tunable H_2S releasing profiles have been achieved. Compared to donor alone, H_2S-fibers have demonstrated prolonged and evenly distributed H_2S release. Furthermore, we investigated the cytoprotective effects of H_2S-fibers against H_2O_2 induced cell injuries. Our data demonstrated that H_2S-fibers released H_2S to the cells and significantly decreased ROS production in H_2O_2 treated cells, thus protecting cells from H_2O_2 induced oxidative damage. Finally, we found that H_2S-fibers can support the proliferation of 3T3 cells and promote the expression of wound healing related genes. Therefore, we anticipate that our H_2S-fibers could be potentially used in skin tissue engineering and a broad range of other biomedical applications.

Supplementary Material

Refer to Web version on PubMed Central for supplementary material.

Acknowledgments

This work was financially supported by the South Carolina EPSCoR-GEAR grant. M.X. thanks American Chemical Society Teva USA Scholar Grant and the NIH (R01HL116571). In addition, the authors would like to acknowledge Mr. Liang Yuan for his help with the FTIR analyses.

References

1. Abe K, Kimura H. The possible role of hydrogen sulfide as an endogenous neuromodulator. J Neurosci. 1996; 16:1066–71. [PubMed: 8558235]
2. Li L, Rose P, Moore PK. Hydrogen Sulfide and Cell Signaling. Annual Review of Pharmacology and Toxicology. 2011; 51:169–87.
3. Meister A, Fraser PE, Tice SV. Enzymatic Desulfuration of Beta-Mercaptopyruvate to Pyruvate. J Biol Chem. 1954; 206:561–75. [PubMed: 13143015]
4. Cavallini D, Mondovi B, De Marco C, Scioscia-Santoro A. The mechanism of desulphhydration of cysteine. Enzymologia. 1962; 24:253–66. [PubMed: 13877466]
5. Braunste, Ae; Goryache, Ev; Tolosa, EA.; Willhard, Ih; Yefremov, Ll. Specificity and Some Other Properties of Liver Serine Sulphhydrase - Evidence for Its Identity with Cystathionine Beta-Synthase. Biochim Biophys Acta. 1971; 242:247. [PubMed: 5121611]
6. Whiteman M, Le Trionnaire S, Chopra M, Fox B, Whatmore J. Emerging role of hydrogen sulfide in health and disease: critical appraisal of biomarkers and pharmacological tools. Clin Sci (Lond). 2011; 121:459–88. [PubMed: 21843150]
7. Lefer DJ. A new gaseous signaling molecule emerges: cardioprotective role of hydrogen sulfide. Proc Natl Acad Sci U S A. 2007; 104:17907–8. [PubMed: 17991773]
8. Song ZJ, Ng MY, Lee ZW, Dai W, Hagen T, Moore PK, et al. Hydrogen sulfide donors in research and drug development. Medchemcomm. 2014; 5:557–70.
9. Hasegawa U, van der Vlies AJ. Design and synthesis of polymeric hydrogen sulfide donors. Bioconjug Chem. 2014; 25:1290–300. [PubMed: 24942989]

10. DeLeon ER, Stoy GF, Olson KR. Passive loss of hydrogen sulfide in biological experiments. Anal Biochem. 2012; 421:203–7. [PubMed: 22056407]
11. Li L, Whiteman M, Guan YY, Neo KL, Cheng Y, Lee SW, et al. Characterization of a novel, water-soluble hydrogen sulfide-releasing molecule (GYY4137): new insights into the biology of hydrogen sulfide. Circulation. 2008; 117:2351–60. [PubMed: 18443240]
12. Benavides GA, Squadrito GL, Mills RW, Patel HD, Isbell TS, Patel RP, et al. Hydrogen sulfide mediates the vasoactivity of garlic. Proc Natl Acad Sci U S A. 2007; 104:17977–82. [PubMed: 17951430]
13. Distrutti E, Sediari L, Mencarelli A, Renga B, Orlandi S, Russo G, et al. 5-Amino-2-hydroxybenzoic acid 4-(5-thioxo-5H-[1,2]dithiol-3yl)-phenyl ester (ATB-429), a hydrogen sulfide-releasing derivative of mesalamine, exerts antinociceptive effects in a model of postinflammatory hypersensitivity. J Pharmacol Exp Ther. 2006; 319:447–58. [PubMed: 16855178]
14. Martelli A, Testai L, Citi V, Marino A, Pugliesi I, Barresi E, et al. Arylthioamides as H2S Donors: l-Cysteine-Activated Releasing Properties and Vascular Effects in Vitro and in Vivo. ACS Med Chem Lett. 2013; 4:904–8. [PubMed: 24900583]
15. Zhao Y, Wang H, Xian M. Cysteine-activated hydrogen sulfide (H2S) donors. J Am Chem Soc. 2011; 133:15–7. [PubMed: 21142018]
16. Venugopal J, Low S, Choon AT, Ramakrishna S. Interaction of cells and nanofiber scaffolds in tissue engineering. J Biomed Mater Res B Appl Biomater. 2008; 84:34–48. [PubMed: 17477388]
17. Liu W, Thomopoulos S, Xia Y. Electrospun nanofibers for regenerative medicine. Adv Healthc Mater. 2012; 1:10–25. [PubMed: 23184683]
18. Chen M, Li YF, Besenbacher F. Electrospun Nanofibers-Mediated On-Demand Drug Release. Adv Healthc Mater. 2014; 3:1721–32. [PubMed: 24891134]
19. Casper CL, Yamaguchi N, Kiick KL, Rabolt JF. Functionalizing electrospun fibers with biologically relevant macromolecules. Biomacromolecules. 2005; 6:1998–2007. [PubMed: 16004438]
20. Nie H, Soh BW, Fu YC, Wang CH. Three-dimensional fibrous PLGA/HAp composite scaffold for BMP-2 delivery. Biotechnol Bioeng. 2008; 99:223–34. [PubMed: 17570710]
21. Eap S, Becavin T, Keller L, Kokten T, Fioretti F, Weickert JL, et al. Nanofibers Implant Functionalized by Neural Growth Factor as a Strategy to Innervate a Bioengineered Tooth. Advanced Healthcare Materials. 2014; 3:386–91. [PubMed: 24124118]
22. Luu YK, Kim K, Hsiao BS, Chu B, Hadjiargyrou M. Development of a nanostructured DNA delivery scaffold via electrospinning of PLGA and PLA-PEG block copolymers. J Control Release. 2003; 89:341–53. [PubMed: 12711456]
23. Coneski PN, Nash JA, Schoenfisch MH. Nitric Oxide-Releasing Electrospun Polymer Microfibers. ACS Applied Materials & Interfaces. 2011; 3:426–32. [PubMed: 21250642]
24. Koh A, Carpenter AW, Slomberg DL, Schoenfisch MH. Nitric Oxide-Releasing Silica Nanoparticle-Doped Polyurethane Electrospun Fibers. ACS Applied Materials & Interfaces. 2013; 5:7956–64. [PubMed: 23915047]
25. Wold KA, Damodaran VB, Suazo LA, Bowen RA, Reynolds MM. Fabrication of biodegradable polymeric nanofibers with covalently attached NO donors. ACS Appl Mater Interfaces. 2012; 4:3022–30. [PubMed: 22663769]
26. Bohlender C, Wolfram M, Goerls H, Imhof W, Menzel R, Baumgaertel A, et al. Light-triggered NO release from a nanofibrous non-woven. J Mater Chem. 2012; 22:8785–92.
27. Liu HA, Balkus KJ. Novel Delivery System for the Bioregulatory Agent Nitric Oxide. Chem Mater. 2009; 21:5032–41.
28. Olson KR. The therapeutic potential of hydrogen sulfide: separating hype from hope. Am J Physiol-Reg I. 2011; 301:R297–R312.
29. Hsiao ST, Dilley RJ, Dusting GJ, Lim SY. Ischemic preconditioning for cell-based therapy and tissue engineering. Pharmacol Therapeut. 2014; 142:141–53.
30. Foley DP, Chari RS. Ischemia-reperfusion injury in transplantation: novel mechanisms and protective strategies. Transplantation Reviews. 2007; 21:43–53.

31. Whiteman M, Moore PK. Hydrogen sulfide and the vasculature: a novel vasculoprotective entity and regulator of nitric oxide bioavailability ? J Cell Mol Med. 2009; 13:488–507. [PubMed: 19374684]
32. Feng S, Duan X, Lo PK, Liu S, Liu X, Chen H, et al. Expansion of breast cancer stem cells with fibrous scaffolds. Integr Biol (Camb). 2013; 5:768–77. [PubMed: 23529778]
33. Peng B, Chen W, Liu C, Rosser EW, Pacheco A, Zhao Y, et al. Fluorescent probes based on nucleophilic substitution-cyclization for hydrogen sulfide detection and bioimaging. Chem Eur J. 2014; 20:1010–6. [PubMed: 24339269]
34. Cipitria A, Skelton A, Dargaville TR, Dalton PD, Hutmacher DW. Design, fabrication and characterization of PCL electrospun scaffolds-a review. J Mater Chem. 2011; 21:9419–53.
35. Beachley V, Wen X. Effect of electrospinning parameters on the nanofiber diameter and length. Materials Science and Engineering: C. 2009; 29:663–8. [PubMed: 21461344]
36. Zan X, Feng S, Balizan E, Lin Y, Wang Q. Facile method for large scale alignment of one dimensional nanoparticles and control over myoblast orientation and differentiation. ACS Nano. 2013; 7:8385–96. [PubMed: 24004197]
37. Li Y, Huang G, Zhang X, Wang L, Du Y, Lu TJ, et al. Engineering cell alignment in vitro. Biotechnol Adv. 2014; 32:347–65. [PubMed: 24269848]
38. Saha S, Duan X, Wu L, Lo PK, Chen H, Wang Q. Electrospun fibrous scaffolds promote breast cancer cell alignment and epithelial-mesenchymal transition. Langmuir. 2012; 28:2028–34. [PubMed: 22182057]
39. Kimura Y, Goto YI, Kimura H. Hydrogen Sulfide Increases Glutathione Production and Suppresses Oxidative Stress in Mitochondria. Antioxid Redox Sign. 2010; 12:1–13.
40. Foster JC, Powell CR, Radzinski SC, Matson JB. S-aroylthiooximes: a facile route to hydrogen sulfide releasing compounds with structure-dependent release kinetics. Org Lett. 2014; 16:1558–61. [PubMed: 24575729]
41. Kleinman WA, Richie JP Jr. Status of glutathione and other thiols and disulfides in human plasma. Biochem Pharmacol. 2000; 60:19–29. [PubMed: 10807941]
42. Chen SC, Huang XB, Cai XM, Lu J, Yuan J, Shen J. The Influence of Fiber Diameter of Electrospun Poly(lactic acid) on Drug Delivery. Fibers and Polymers. 2012; 13:6.
43. Zong X, Bien H, Chung C, Yin L, Fang D, Hsiao B, et al. Electrospun fine-textured scaffolds for heart tissue constructs. Biomaterials. 2005; 26:5330–8. [PubMed: 15814131]
44. Calvert JW, Elston M, Nicholson CK, Gundewar S, Jha S, Elrod JW, et al. Genetic and pharmacologic hydrogen sulfide therapy attenuates ischemia-induced heart failure in mice. Circulation. 2010; 122:11–9. [PubMed: 20566952]
45. King AL, Lefer DJ. Cytoprotective actions of hydrogen sulfide in ischaemia-reperfusion injury. Exp Physiol. 2011; 96:840–6. [PubMed: 21666033]
46. Henderson PW, Singh SP, Belkin D, Nagineni V, Weinstein AL, Weissich J, et al. Hydrogen sulfide protects against ischemia-reperfusion injury in an in vitro model of cutaneous tissue transplantation. J Surg Res. 2010; 159:451–5. [PubMed: 19811790]
47. Ricotti L, Polini A, Genchi GG, Ciofani G, Iandolo D, Vazao H, et al. Proliferation and skeletal myotube formation capability of C2C12 and H9c2 cells on isotropic and anisotropic electrospun nanofibrous PHB scaffolds. Biomed Mater. 2012; 7:035010. [PubMed: 22477772]
48. Slezak J, Tribulova N, Pristacova J, Uhrik B, Thomas T, Khaper N, et al. Hydrogen peroxide changes in ischemic and reperfused heart. Cytochemistry and biochemical and X-ray microanalysis. Am J Pathol. 1995; 147:772–81. [PubMed: 7677188]
49. Law CH, Li JM, Chou HC, Chen YH, Chan HL. Hyaluronic acid-dependent protection in H9C2 cardiomyocytes: a cell model of heart ischemia-reperfusion injury and treatment. Toxicology. 2013; 303:54–71. [PubMed: 23178681]
50. Nisbet DR, Forsythe JS, Shen W, Finkelstein DI, Horne MK. Review paper: a review of the cellular response on electrospun nanofibers for tissue engineering. J Biomater Appl. 2009; 24:7–29. [PubMed: 19074469]
51. Raedschelders K, Ansley DM, Chen DD. The cellular and molecular origin of reactive oxygen species generation during myocardial ischemia and reperfusion. Pharmacol Ther. 2012; 133:230–55. [PubMed: 22138603]

52. Sun WH, Liu F, Chen Y, Zhu YC. Hydrogen sulfide decreases the levels of ROS by inhibiting mitochondrial complex IV and increasing SOD activities in cardiomyocytes under ischemia/reperfusion. Biochem Biophys Res Commun. 2012; 421:164–9. [PubMed: 22503984]

53. Bindokas VP, Jordan J, Lee CC, Miller RJ. Superoxide production in rat hippocampal neurons: selective imaging with hydroethidine. J Neurosci. 1996; 16:1324–36. [PubMed: 8778284]

54. Yates CC, Hebda P, Wells A. Skin wound healing and scarring: fetal wounds and regenerative restitution. Birth Defects Res C Embryo Today. 2012; 96:325–33. [PubMed: 24203921]

55. Nedelec B, Ghahary A, Scott PG, Tredget EE. Control of wound contraction. Basic and clinical features. Hand Clin. 2000; 16:289–302. [PubMed: 10791174]

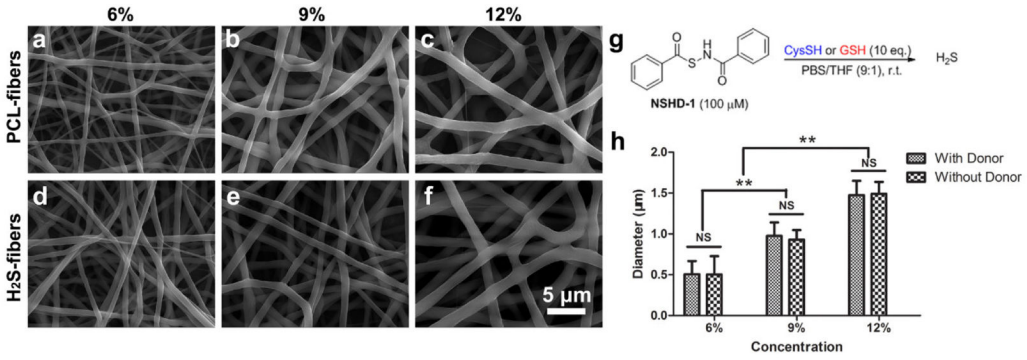

Figure 1.

SEM images of H_2S-fibers (a–c) and PCL-fibers (d–f) generated from 6%, 9% and 12% w/v solutions (from left to right). All images share the same scale bar in (f). (g) The H_2S donor, NSHD-1, releases H_2S in the presence of cysteine o GSH. (h) Fiber diameters plot as a function of solution concentrations. The dopant, NSHD1, has no obvious effect on fiber diameters. All data are expressed as mean ± SE, and statistical significance was assessed using two-way ANOVA. ** indicates $P < 0.05$; NS indicates not significant ($n = 200$).

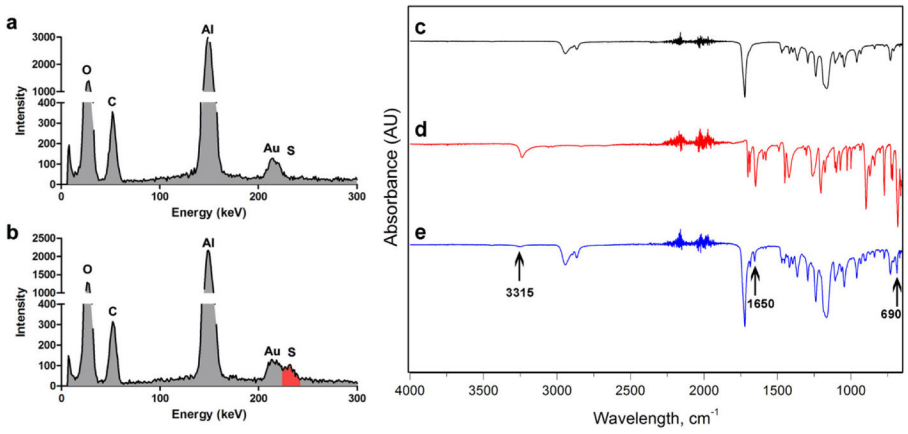

Figure 2.

EDX and FT-IR analysis of PCL-fibers and H_2S-fibers. EDX spectrum shows the comparison between PCL-fibers (a) and H_2S-fibers (b). The red color indicates the sulfur peak. FT-IR spectrum of (c) PCL-fibers, (d) NSHD1, and (e) H_2S-fibers.

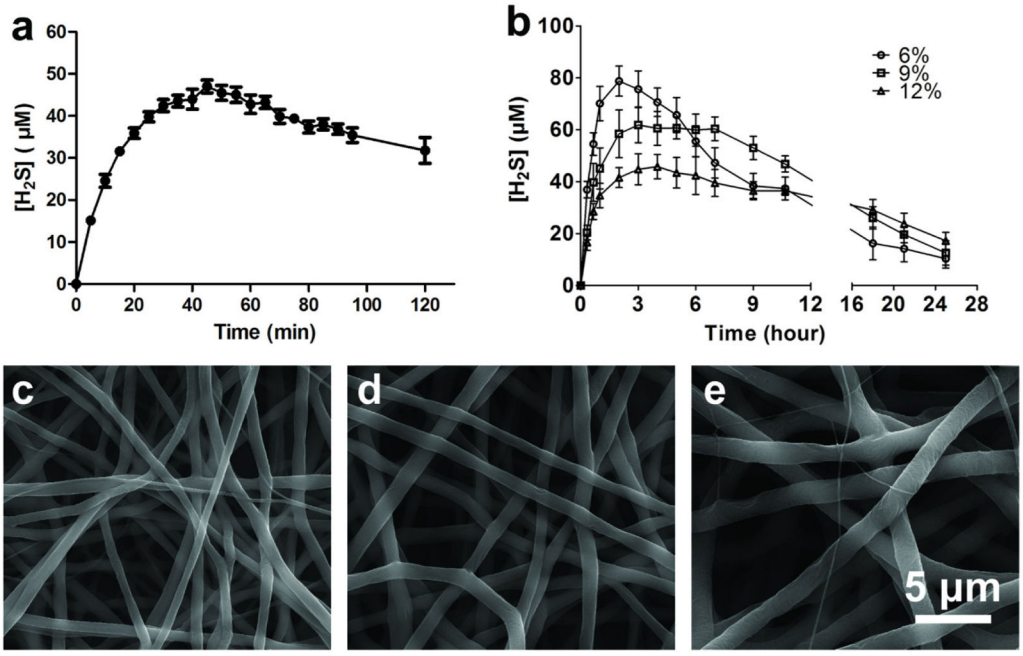

Figure 3.

(a) H_2S release kinetics of NSHD1 (100 μM) in the presence of 1 mM cysteine. (b) H_2S release kinetics of H_2S-fibers generated from 6%, 9% and 12% w/v H_2S donor/PCL solutions (H_2S donor:PCL = 1:10) in the presence of 1 mM cysteine. All data are expressed as mean ± SEM (n = 3). SEM images of H_2S-fibers generated from 6% (c), 9% (d) and 12% (e) w/v H_2S donor/PCL solutions after in vitro release in pH =7.4 buffer solutions for 48 h.

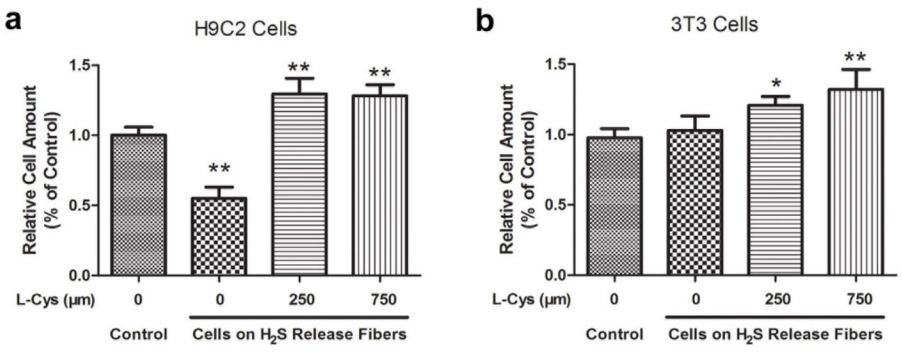

Figure 4.

Effects of H_2S-fibers on cell viability. H9c2 cells (a) and NIH 3T3 cells (b) were cultured in fibrous scaffolds in presence of cysteine at indicated amount for 24 hours. CellTiter-Blue assay was performed to measure cell viability. All data were expressed as the mean ± SEM (n = 6). * indicates $P < 0.05$ vs. Control group (cells in PCL fibers). ** indicates $P < 0.01$ vs. Control group.

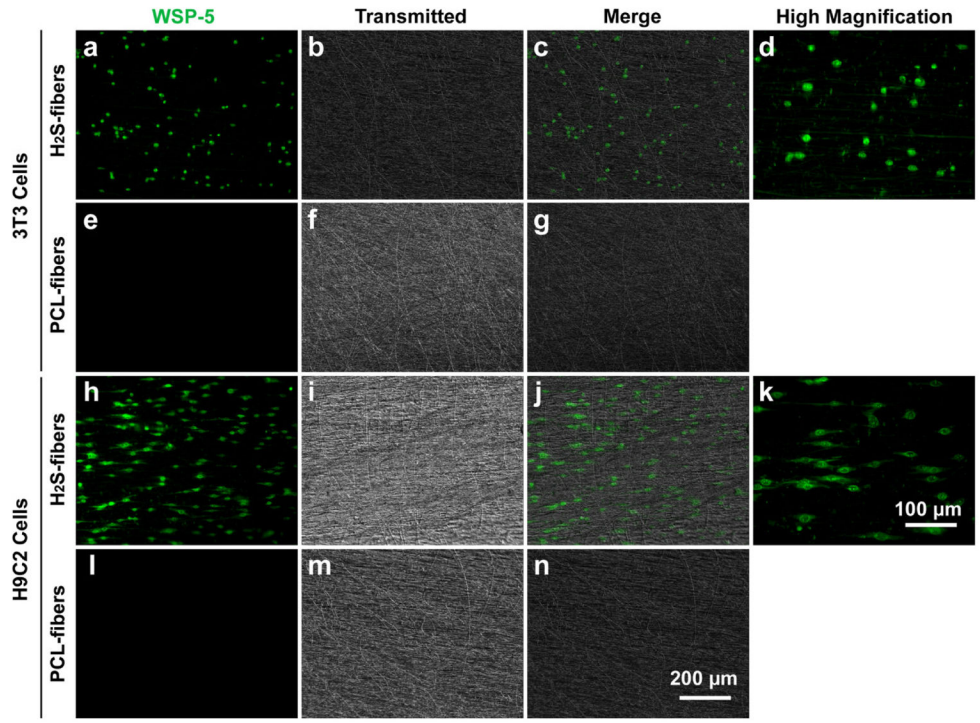

Figure 5.

H_2S detection in NIH 3T3 cells and H9c2 cells. NIH 3T3 (top 2 rows) and H9c2 cells (bottom two rows) were cultured on H_2S-fibers (first and third rows) or PCL-fibers (second and last rows) for 12 hours, 100 μM of a H_2S fluorescent probe (WSP-5, green channel) was used to detect H_2S production in cells. (d) and (k) are higher magnification view of (a) and (h), respectively. (a–c), (e–g), (h–j), and (l–n) share the scale bar as in (n). (d) and (k) share the scale bar in (k).

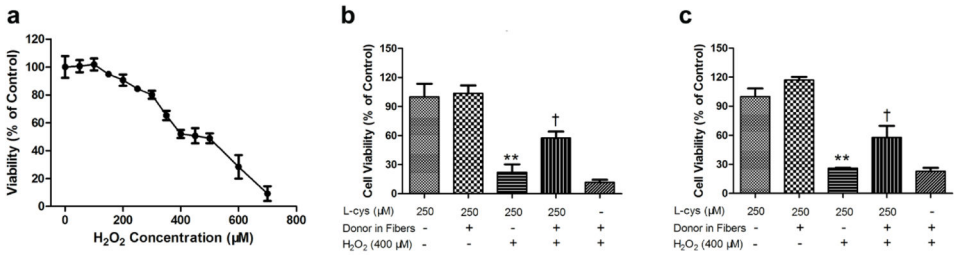

Figure 6.

H_2S-fibers protected cells from H_2O_2 induced oxidative injury. (a) H9c2 cells were treated with H_2O_2 at indicated concentrations for 24 h. Before treated with 400 μM H_2O_2 for 24 h, H9c2 (b) and NIH 3T3 (c) were cultured in either PCL-fibers (Donor −) or H_2S-fibers (Donor +) with or without 250 μM cysteine. Cell viability was measured by CellTiter-Blue assay. All data were shown as the mean ± SEM (n = 6). ** indicates $P<0.01$ vs. Control group (cells in PCL-fibers without H_2O_2 treatment). † indicates $P<0.01$ vs. cells in PCL-fibers with H_2O_2 treatment group.

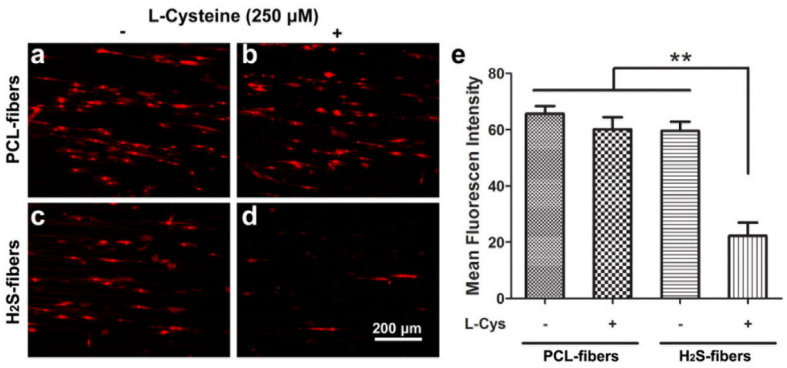

Figure 7.

H_2S-fibers prevented reactive oxygen species (ROS) production in H_2O_2 treated H9c2 cells. Representative images of DHE-fluorescence intensity were taken 2 h after H_2O_2 treatment for cells in PCL-fibers (a–b) or H_2S-fibers (c–d) with (right column) or without 250 μM (left column) cysteine. (e) H_2S-fibers significantly decreased DHE-fluorescence intensity in H9c2 cells in presence of 250 μM cysteine compared to other group (n = 20). All data were expressed as the mean ± SEM. ** indicates $P < 0.01$.

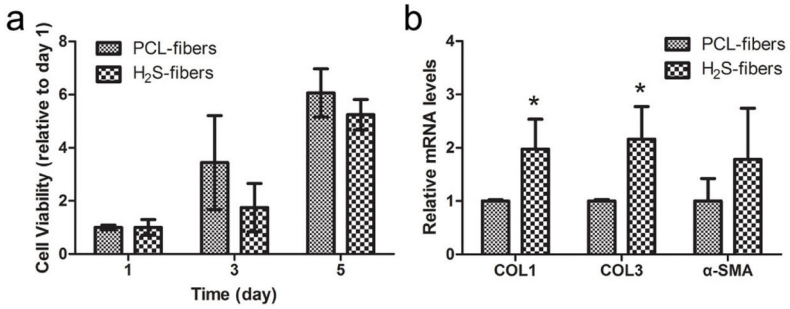

Figure 8.

H_2S-fibers for wound healing. (a) The proliferation of 3T3 cells in H_2S-fibers and PCL fibers (n = 6). (b) Expression of wound healing related genes (n = 3). All data were expressed as the mean ± SEM. ** indicates $P < 0.05$.